Wear and Lifespan Evaluation of solid lubricant in Rotary Compressors Operating in a Refrigerant Oil Environment

Jaesang Yoo[1], Si-Geun Choi[1], Jong-Hyoung Kim[1], InKang Heo[1], SooDol Park[2], Byunghyun Kim[2], JunPyo Lee[2], Jin-Young Park[1*]

[1] Korea Institute of Industrial Technology, Korea, Republic of (South Korea)
[2] Samsung Electronics Co., Ltd. / Digital Appliances / Compressor & Motor Business Team, Republic of (South Korea)
* Corresponding Author: jinypark@kitech.re.kr

ABSTRACT

The evaluation of the wear and lifespan of solid lubricants is derived in the components of rotary compressors operating in a refrigerant oil environment. Unlike conventional mechanical components that have established lifespan equations based on operating conditions, this research focuses on studying failure caused by mechanical wear. The objective is to derive a wear life equation according to various test conditions, and friction experiments were proceeded for this purpose. Considering the load application method of compressor, a pin-on-disc friction test method was employed, utilizing coated specimens to simulate real surface conditions. The friction tests were conducted, and the wear volume was measured at regular intervals during the test cycles. By employing lifespan calculation equations, the point at which the coating layer was delaminated could be determined. To ensure coating delamination, harsh conditions were implemented, surpassing conventional operating conditions. These harsh conditions were determined by conducting preliminary experiments, varying the parameters of load, speed, and temperature. The result is to derive the lifespan equation of coating delamination, comparing the acceleration life of compressor, lifespan of bearing in rotary compressor, and the lifespan with the experimentally obtained equation, and thereby assessing the differences. Additionally, the study aims to develop an evaluation method to investigate the effects of using different oil types. The findings will contribute to a better understanding of failure mechanisms and the development of evaluation techniques for rotary compressors operating in refrigerant oil environments.

1. INTRODUCTION

Wear of mechanical devices or parts can be caused by various factors, and the part where wear occurs the most is one of the important research topics. Compressors can cause performance degradation and failure when parts are worn out due to long-term use or improper maintenance. As this directly affects productivity and safety, research and preventive measures for wear are emerging as important issues. In addition, the use of harmful substances including CFC and HCFC has been banned due to environmental issues, and new refrigerants that can replace HFC have to be developed and applied. Therefore, it is necessary to study how the wear-out area acts in various refrigerant environments (Yun 2000, Wu et al. 2017, Wu et al. 2016, Xu et al. 2013). Compressor wear can be caused by several factors. Parts inside the compressor are exposed to periodic friction and thermal changes, so it is necessary to consider condition changes such as operating load, speed, temperature, etc. Also, the material and shape of the part can affect the wear. This is because the material of the part directly affects the durability and resistance to wear, and the shape determines the contact area, strength, etc. of the exposed part. Studies on wear and friction are an essential part of evaluating the safety and reliability of compressors, but they are quite inefficient in terms of time. In addition, limitations such as actual environmental simulation reduce the efficiency of the test and use accelerated test to overcome these shortcomings (Jeon and Lee 2013, Hoess et al. 2022). Accelerated testing can help predict the lifespan of a product and reduce the time required for product development and production. This study deals with the friction between the shaft and the journal inside the rotary compressor. The rotating shaft and cam are supported by two fixed journals, and the sliding friction occurs at the contact area. The schematic view is shown in Figure 1. The shaft surface is treated with a solid lubricant coating, and experiments were conducted using materials that simulate the contact counterparts.

Since friction occurs in a refrigerant environment, refrigerant oil was used as the lubricant. Wear phenomena do not occur properly under actual conditions of pressure, speed, and temperature; therefore, accelerated conditions based on actual conditions were derived for testing. The test results provided data on the wear area according to the cycle, from which a wear map and a graph predicting wear life were derived. This allows for the selection of test condition areas applicable to the said sliding bearing, setting the design area through prediction of bearing constant values. Further research will explore the possibility of applying this to new refrigerants and sliding bearings through validation tests with individual component testing.

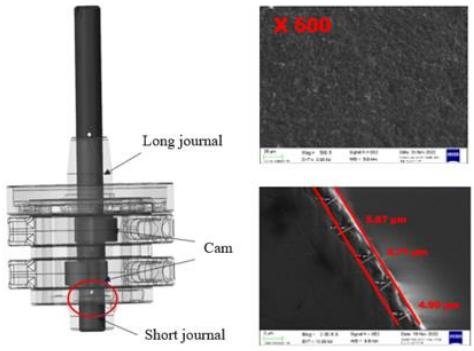

Figure 1: Schematic view of the rotating shaft and cam with journal inside a rotary compressor. The area of red circled is targeted for friction analysis.

2. METHODS AND MATERIALS

The target evaluation part is the part where the shaft connected to the motor and the supporting bearing contact each other. The centrifugal force caused by the rotation of the crankshaft applies a radial load to the supporting bearing and friction occurs between the bearing in contact with the solid lubrication coating on the shaft surface. A friction test was set in consideration of the operating environment of the compressor. To derive the wear test conditions for the accelerated test, a process of setting conditions for load, speed, and temperature was conducted. The accelerated conditions were set towards the direction indicating higher friction coefficients in each condition area. Pressure conditions were harshly set in double or more, considering that the average surface pressure applied during real world operation condition was about 3.2 MPa. As for the speed, conditions were decided based on the Stribeck diagram of each test condition. Therefore, preliminary tests of pin-on-disc stribeck cureve test were done for 3 times of repetitive tests of load, temperature conditions. The temperature was designated in the range between 70 degrees and 130 degrees in consideration of the actual compressor operating environment. As the temperature increases, the viscosity of the refrigerant decreases, so the high temperature condition is set as severe conditions. Pin-on-disc method was determined and the result was analyzed by measuring the amount of wear for each test condition. Detailed test conditions are indicated in Table 1. The friction test and precision measurement were conducted with TE92-HS by Phoenix, VK-3000 by KEYENCE, and SV-3200S4 by Mitutoyo. All conditions were tested and precisely measured in 15,000 cycle increments, with a total of up to 75,000 cycles conducted. For the specimen, a solid lubricant coating was applied to a 60 mm diameter disk specimen, and an 8 mm diameter cast iron pin specimen was used as a counterpart.

Table 1: Friction test conditions and properties.

Lubricants	Test Conditions		
	Load (MPa)	**Speed (RPM)**	**Temeprature (℃)**
Refrigerant Oil A	5.97	250	70
			100
			130
		600	70
			100
			130
		950	70
			100
			130
	9.95	250	70
			100
			130
		600	70
			100
			130
		950	70
			100
			130
	13.93	250	70
			100
			130
		600	70
			100
			130
		950	70
			100
			130
	Distance	Total 75,000cycles for 5 tests (15,000 for 1 test)	

The detailed measurement was accumulated by measuring before and after the test. For the amount of wear, the area of the wear track of the disk specimen was analyzed, and for the roughness, the wear track and the surface of the relative were measured using the ISO1997 standard. The precise measurement was measured by 4 parts per specimen to derive the average value and used for calculation (Figure 2). The wear mechanism and the direction of wear progress were analyzed through the imaging of the surface shape, and reliability analysis was attempted through the wear amount graph. In the case of the reliability evaluation, considering that the form of friction generated by the shaft and bearing is a journal bearing, the Petroff equation was derived and the bearing integer value was derived and linked. In addition, in addition to the analysis through these test results, a life equation using the life prediction equation of the compressor itself was derived and compared with each other.

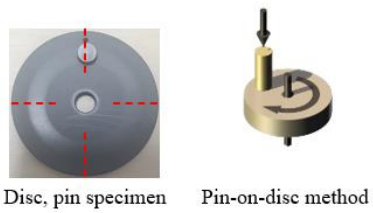

Figure 2: Test specimen of disc and pin (left), and schematic view of pin-on-disc test method. Precise measurements were conducted in the area marked with a red dashed line.

3. TEST RESULTS

3. Friction test results

Tests were conducted with each condition, and wear maps were derived for each temperature. When the horizontal axis is expressed as load, the vertical axis is velocity, and the color change of the graph is expressed as the amount of wear, the result as shown in Figure 3 was obtained. Each graph A, B, and C is divided by temperature, and overall, the more severe the condition, the higher the wear rate.

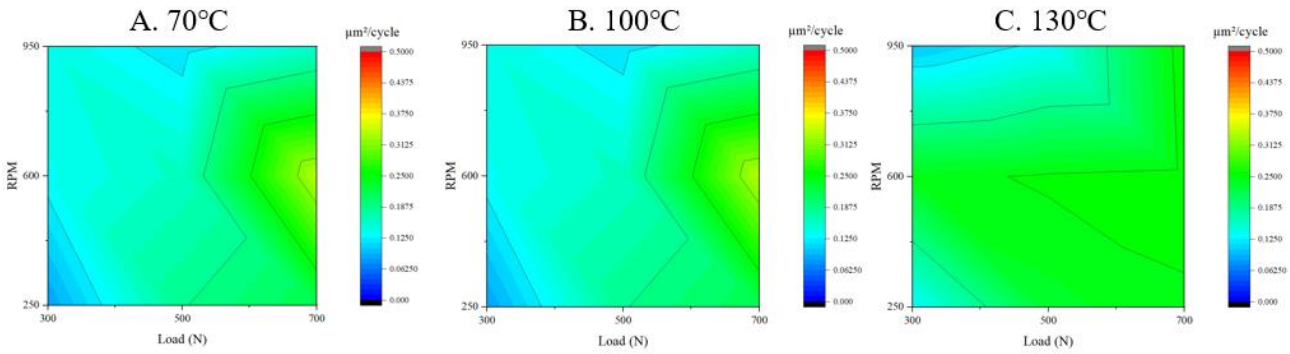

Figure 3: Wear map according to each test temperature conditions

4. DISCUSSION

Based on these results, variable integration for static data analysis was implemented. The friction point viewed as a target in this study can be replaced by a journal bearing due to wear between the shaft and the sliding bearing. In addition, bearing integers can be applied because it is a lubricating environment where refrigerant enters. The bearing integer can be expressed as the applied pressure, the rotation speed of the shaft (rpm), and the viscosity value of the fluid in contact. In typical journal bearing, assuming that the viscosity of the fluid is η, the speed of the fluid is u, the thickness of the oil film is δ, and the bearing rotation speed is N. Then the fluid shear stress at a certain y axis can be expressed as follows.

$$\tau = \eta \frac{du}{dy} \approx \eta \frac{u}{\delta} = \eta \frac{1}{\delta} \left(\frac{N}{60} 2\pi r\right) \tag{1}$$

Since the area where the stress is applied is expressed as Equation 2, the fluid shear torque comes out as Equation 3, where l is axial bearing length, r is bearing radius.

$$A = 2\pi l \tag{2}$$

$$\text{Fluid shear Torque} = \tau A r = \eta \frac{1}{\delta} \left(\frac{N}{60} 2\pi r\right) \times (2\pi l) \times r \tag{3}$$

The pressure of the bearing p can be expressed in terms of bearing load F, and applied area (Equation 4). And the friction force can be defined in terms of pressure (Equation 5). The friction torque from the bearing load can be expressed as Equation 6.

$$p = \frac{F}{2rl} \tag{4}$$

$$\text{Friction Force} = \mu F = \mu \times 2plr \tag{5}$$

$$\text{Torque} = \mu F r = 2\mu plr^2 \tag{6}$$

Since the fluid shear torque and the friction torque derived from the load are same, the Equation 3 and Equation 6 can be combined.

$$\mu = \frac{\pi^2}{30} \cdot \eta \frac{N}{p} \cdot \frac{r}{\delta} \tag{7}$$

Meanwhile, due to the difference between the wear environment of the actual part and the experimental environment, bearing modulus cannot be matched simply by load, speed, and fluid viscosity values. In order to derive the related equation, a theory related to the induction of bearing modulus is required. The bearing modulus can be derived by the Petroff equation, which represents the form of the first-order equation in which the bearing modulus is entered as a variable for the value of the coefficient of friction. Here, the constant value including the gap ratio is attached as a coefficient, and the gap ratio can be expressed as the thickness of the bearing gap and the oil film. Using the Petroff equation principle below, a method of applying the same to the experimental environment was sought. Figure 4A represents the typical journal bearing lubricant gap (yellow region). The Petroff equation can be derived with the corresponding figure 4A. Figure 4B shows a schematic diagram of the pin-on-disk friction test and has the same lubrication gap (yellow area). Figure 4C is a schematic diagram showing the fluid flowing in the gap. If the direction perpendicular to the fluid flow direction is y, the fluid flow rate of the rotating surface is fast. Applying the principle used in Petroff's equation to the pin-on-disk test can obtain the same equation as Equation 14.

The commonly used Petroff equation was derived in Equation 7. By using the same principle, the equation was applied to the test method. The below is a theoretical equation applied to the pin-on-disk method. Assume the viscosity of the fluid is η^*, the speed of the fluid is u^*, the thickness of the oil film is δ^*, the rotating speed of the tester is N^*, and the distance from the center of the pin is R. Then the fluid shear stress at a certain y axis can be expressed as follows.

$$\tau^* = \eta^* \frac{du^*}{dy} \approx \eta^* \frac{u^*}{\delta^*} = \eta^* \frac{1}{\delta^*} \left(\frac{N^*}{60} 2\pi R\right) \tag{8}$$

As the pressure is applied to the pin, the area A^* is equal to the size of the pin (d=pin diameter). Then the fluid shear torque can be written like Equation 10.

$$A^* = \pi \frac{d^2}{4} \tag{9}$$

$$\tau^* A^* R = \eta \frac{1}{\delta} \left(\frac{N}{60} 2\pi r\right) \times (2\pi l) \times r \tag{10}$$

The pressure of the bearing p can be expressed in terms of bearing load F^*, and applied area (Equation 9). And the friction force can be defined in terms of pressure (Equation 12). The friction torque from the bearing load can be expressed as Equation 13.

$$p^* = \frac{F^*}{A^*} \tag{11}$$

$$\text{Friction Force} = \mu^* F^* = \mu^* \times A^* p^* \tag{12}$$

$$\text{Torque} = \mu^* F R = \mu^* A^* p^* R \tag{13}$$

Since the fluid shear torque and the friction torque derived from the load are same, the Equation 10 and Equation 13 can be combined.

$$\mu^* = \frac{\pi}{30} \cdot \eta^* \frac{N^*}{p^*} \cdot \frac{R}{\delta^*} \tag{14}$$

By comparing Equations 7 and 14, the difference between the real bearing and the pin-on disk module can be

theoretically analyzed. For variable unification, the bearing modulus value according to each load, speed, and temperature condition was derived and expressed in Table 2. After integrating each condition into one variable, a graph using the wear amount data was derived in Figure 5. Figure 6 displays the graph of precise measurement results for each disc and pin specimen.

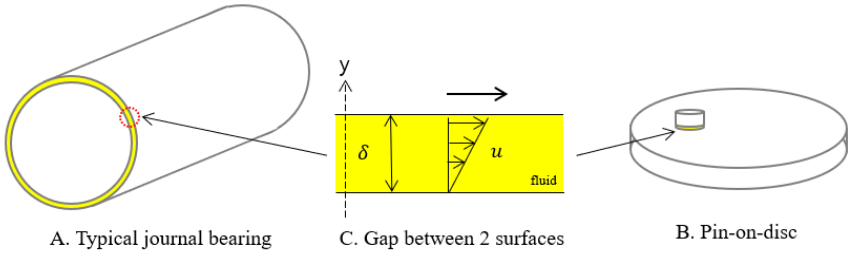

Figure 4: Figure of typical journal bearing (A), pin-on-disk specimen (B), and fluid schematic diagram in contact area (C).

Table 2: Hersey number of each test condition.

Pressure	**RPM**	$\mu\frac{V}{p}$		
		Temperature		
		70℃	**100℃**	**130℃**
5.97MPa	250	7.49E-08	3.11E-08	1.64E-08
	600	1.80E-07	7.47E-08	3.94E-08
	950	2.85E-07	1.18E-07	6.24E-08
9.95 MPa	250	4.49E-08	1.87E-08	9.86E-09
	600	1.08E-07	4.48E-08	2.37E-08
	950	1.71E-07	7.09E-08	3.75E-08
13.93 MPa	250	3.21E-08	1.33E-08	7.04E-09
	600	7.70E-08	3.20E-08	1.69E-08
	950	1.22E-07	5.07E-08	2.68E-08

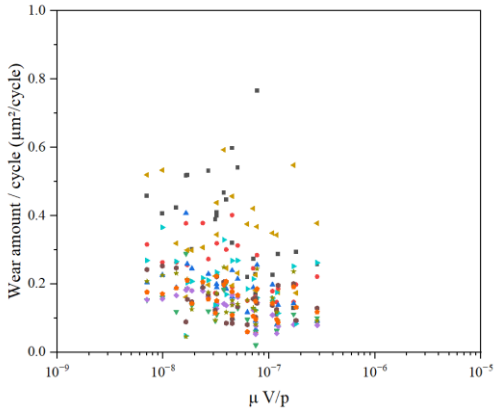

Figure 5: Graph of wear amount per cycle with $\mu\frac{V}{p}$. The horizontal axis integrates load, temperature, and velocity variables into one variable.

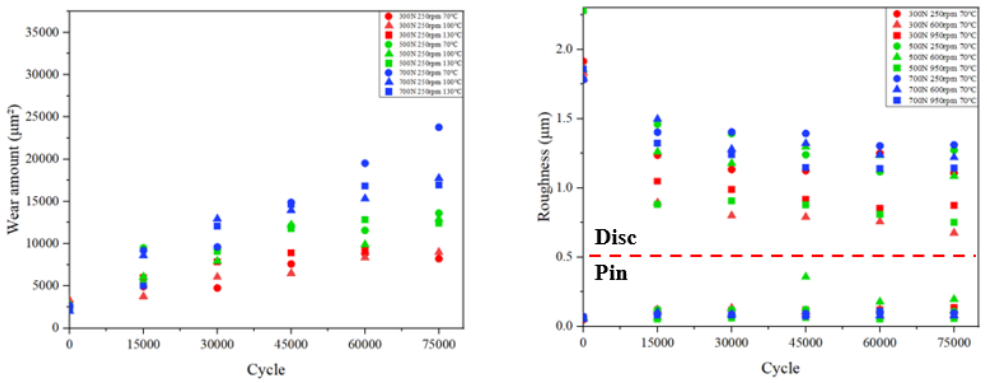

Figure 6: The graph represents the roughness measurement results for both disc and pin specimens under all test conditions. Above the red dashed line indicates the roughness of the disc specimens, while below it represents the roughness of the pin specimens.

4. DISCUSSION

The development of a wear rate versus μV/p graph, derived from the analysis of wear area and cycle data, enables a nuanced understanding of the wear behaviors under varied conditions. The result graph of Figure 6 facilitates the preliminary prediction of lifespan according to specific operational scenarios, aligning with the objective to quantify the durability of solid lubricants within rotary compressors operating in refrigerant oil environments. By correlating wear rate with the product of friction coefficient (μ), velocity (V), and inverse pressure (1/p), this study advances the comprehension of wear mechanisms, offering a pathway to tailor lubrication strategies effectively. The empirical relationship, supported by data visualization, underscores the intricate balance between mechanical interactions and lubricant performance, projecting an innovative methodology for lifespan estimation that mirrors practical wear phenomena.

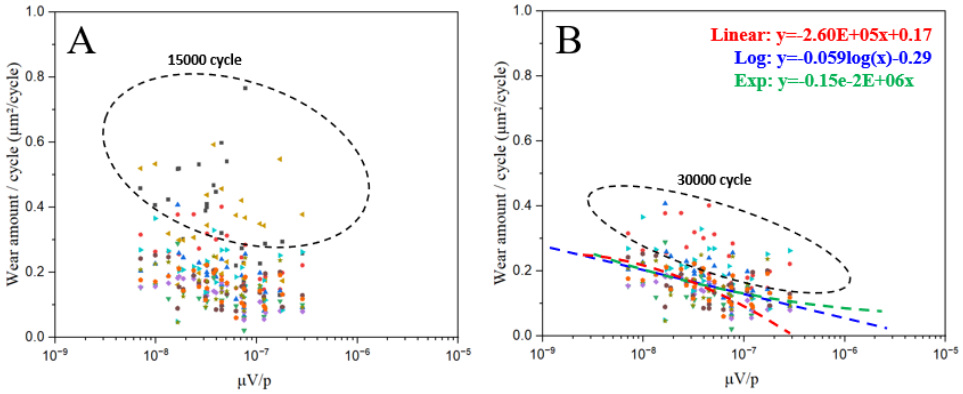

Figure 7: Each graph represents the wear rate at the respective cycle count.

The results of this entire study are shown as one graph in Figure 5 with the large variance of data. Analysis of the corresponding data was performed in Figure 7. Graph 7A shows the results of all test conditions and is circled for the initial cycle section, the 15,000cycle area. Graph B is data excluding 15000 cycle data, and the area corresponding to the 30,000cycle data is circled. The red, blue, and green lines in Figure 7B represent the prediction lines drawn using the data excluding the initial run-in process. The respective equation for these prediction lines is displayed at the top of Graph B. The data area according to each test condition is shown in Figure 8. It is possible to visually see the pattern according to the condition change. The observed range in the graph poses challenges for precise prediction, primarily due to the initial data variability. Notably, data points skewing towards higher values predominantly originate from the initial stages of testing. This trend may reflect the run-in phase, where the disc's initial surface roughness significantly reduces before stabilizing, suggesting a conditioning effect on the wear mechanism. Such observations

are consistent with established theories and empirical studies, which acknowledge the impact of initial wear-in conditions on the long-term wear behavior of mechanical components. For instance, the comprehensive review of various studies, including those related to run-in effects in different friction and wear testing scenarios, provides insights into how materials behave under initial frictional contact and subsequent stabilization (Meng et al. 2022). This phase is crucial for establishing a steady state of wear, where surfaces adapt to generate consistent frictional behavior, thus offering a critical lens through which to evaluate the performance of solid lubricant coatings under variable conditions. The adaptation of the Petroff equation to this study's context underlines the intricacies of correlating pin-on-disc test results to real-world bearing applications. By extending the equation to the experimental setup, a bridge connecting theoretical predictions was crafted with empirical data. The equation's application, which integrates parameters such as static viscosity, fluid velocity, and film thickness, elucidates the relationship between the frictional forces encountered in test scenarios and those in actual compressor bearings. This comparison reveals discrepancies attributable to the simplified assumptions of the testing environment versus the complex dynamics of actual compressor operations. Despite these differences, the equation serves as a foundational tool for extrapolating bearing wear under realistic conditions, thereby enhancing the predictive accuracy of our lifespan models.

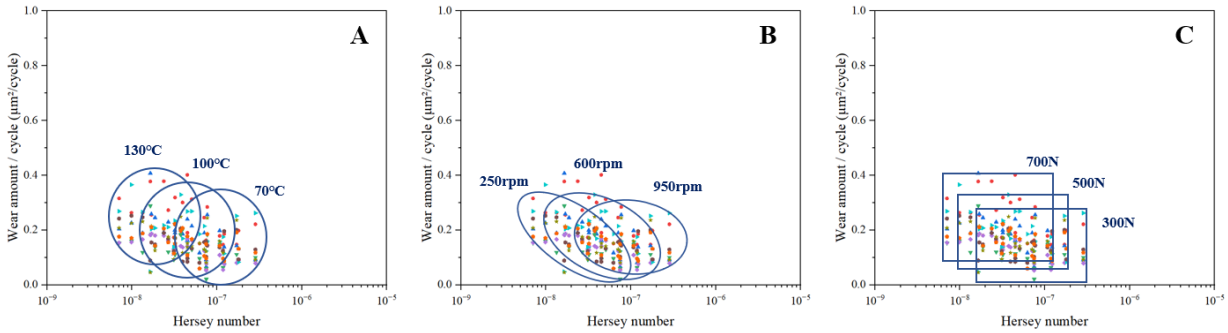

Figure 8: Data area based on temperature (A), speed (B), and load (C).

5. CONCLUSION

The study's exploration into wear mechanisms, facilitated by a solid lubricant in rotary compressors, reveals the multifaceted interactions between material properties, operational conditions, and wear rates. As a result of the experiment, a graph of the wear rate per cycle according to the Hersey number was derived. Through data analysis, it was possible to visually analyze how the wear rate changes according to each test condition and the life prediction line can be derived, which can be used to set the bearing modulus value. The findings not only contribute to the refinement of predictive models for compressor lifespan but also underscore the importance of considering initial wear-in processes in the evaluation of long-term component durability. Furthermore, by bridging theoretical principles with practical testing methodologies, this research amplifies our understanding of lubrication dynamics, paving the way for more reliable and efficient compressor designs.

NOMENCLATURE

η	Static viscosity	(St)
u	Fluid velocity	(mm/s)
p	Average pressure	(Pa)
F	Bearing weight	(N)
N	Rotating speed	(RPM)
δ	Film thickness	(μm)
r	Bearing radius	(mm)
l	Length of bearing	(mm)
μ	Friction coefficient	(–)
η ∗	Static viscosity	(St)
u ∗	Fluid velocity	(mm/s)
p ∗	Average pressure	(Pa)
F ∗	Load	(N)
N ∗	Test speed	(RPM)
δ ∗	Film thickness	(μm)
R	Track radius	(mm)
μ ∗	Friction coefficient	(–)

REFERENCES

K. W. Yun (2000). Failure Modes and Risk Assessment of Rotary Compressor Under Extraordinary Operating Conditions. *ICECP* Paper 1382.

Jianhua Wu, Jie Lin, Ze Zhang, Zhenhua Chen, Jing Xie, Jun Lu, (2017). Experimental investigation of dynamic characteristics of a rotary compressor and its air conditioner using R290 during warm startup. *Appl. Therm. Eng* Volume 125, Pages 1469-1477

J Wu, J Lin, Z Zhang, Z Chen, J Xie, J Lu (2016). Experimental investigation on cold startup characteristics of a rotary compressor in the R290 air-conditioning system under cooling condition. *IJACR* Volume 65, Pages 209-217

X. Xu, Y. Hwang, R. Radermacher, (2013). Performance comparison of R410A and R32 in vapor injection cycles[J]. *Int. J. Refrig.* 36 (3), pp. 892-903

HG Jeon, YZ Lee, (2013). The evaluation of wear life based on accelerated test through analysis of correlation between wear rate and lubricant film parameter. *Tribol. Trans.* Volume 56, Issue 2

Andreas Josef Hoess, Davide Ziviani, Eckhard A Groll, James E Braun, (2022). Development and Application of Accelerated Life Test Cycles for Performance Degradation Study on Water-cooled Variable-speed Screw Compressor Chillers, *International Compressor Engineering Conference* Paper 2786

Yonggang Meng, Jun Xu, Liran Ma, Zhongmin Jin, Braham Prakash, Tianbao Ma & Wenzhong Wang, (2022). A review of advances in tribology in 2020–2021. *Friction* Volume 10, pages 1443–159

ACKNOWLEDGEMENT

This work was supported by the Industry Innovation Infrastructure Program(P0018678) funded by the Ministry of Trade, Industry & Energy(MOTIE, Republic of Korea).

This research was conducted with the support of a private assignment project from Samsung Electronics and the Korea Institute of Industrial Technology. The research team extends deep gratitude for the support provided by both institutions.